

Design of Modular Multimode Cavities

Mikkel Heuck

Department of Electrical and Photonics Engineering
Technical University of Denmark

Lyngby, Denmark
mheu@dtu.dk

Abstract—Resonant enhancement of light-matter interactions is broadly applicable across many device functionalities where reduced energy consumption and footprint are important figures of merit. The increased sensitivity of resonant devices, however, makes both design and fabrication challenging in terms of reliability and yield. Here, we propose a design approach and device architecture that enable devices that have rich and re-configurable spectral responses.

Index Terms—Photonic Integrated Circuits, NEMS, Programmable Photonics, Photonic Crystals.

I. INTRODUCTION

Integrated photonics is attracting an increasing amount of attention because of the potential for harnessing the properties of light to realize complex functionalities in a platform suitable for mass production. Miniaturizing optical components and the accompanying increase in light intensities provide new opportunities for developing devices with unprecedented sensitivity. The most extreme enhancement of light-matter interactions was demonstrated in photonic crystal (PhC) nanocavities [1]. While having received considerable scientific attention, practical applications based on PhC cavities remain missing for two main reasons: 1) Resonant devices have a fundamentally limited operation bandwidth set by their linewidth. 2) Fabrication imperfections or varying operating conditions necessitate fine-tuning of the spectral response across many devices.

Here, we address these challenges by introducing a new device architecture based on modular cavities. As illustrated in Fig. 1, our proposed devices consist of individually programmable mirror modules that are controlled by actuators based on nano-electromechanical systems [2], [3]. The modular structure simultaneously enables a high degree of device programmability and efficient design optimization.

II. TRANSFER MATRIX DESIGN APPROACH

We describe each mirror module of the cavity by a 2-by-2 scattering matrix,

$$\mathbf{S}^{(n)}(\omega) = e^{i\phi_n(\omega)} \begin{bmatrix} ir_n(\omega) & \sqrt{1-r_n(\omega)^2} \\ \sqrt{1-r_n(\omega)^2} & ir_n(\omega) \end{bmatrix}, \quad (1)$$

and extract the real parameters $r_n(\omega)$ and $\phi_n(\omega)$ by comparing to full 3D simulations. Reducing the model to a 1D description drastically reduces the computational resources required to calculate the spectral response of N -section cavities. Knowing $r_n(\omega)$ and $\phi_n(\omega)$ as a function of the applied force, F_n , the

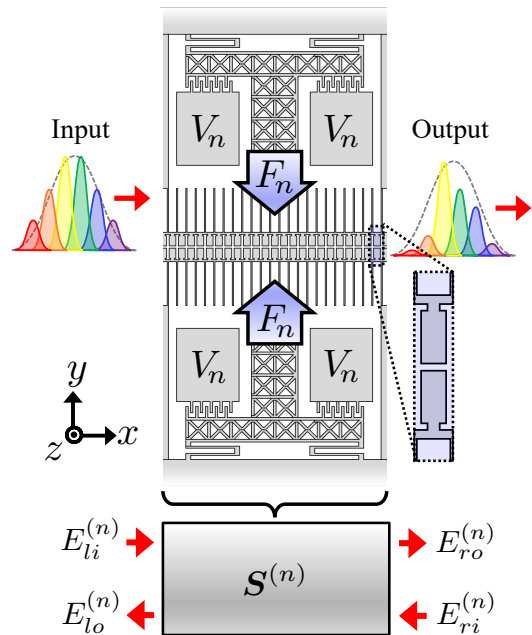


Fig. 1. Sketch of a single cavity module consisting of a PhC slot waveguide connected to comb drive actuators. Adjusting the actuator voltages, V_n , causes a force, F_n , to modify the reflectivity of the module by changing the waveguide gap. The zoom-in shows the geometry of a single unit cell of the PhC waveguide. Each mirror module is described by a scattering matrix, $\mathbf{S}^{(n)}$, that allows efficient modeling and design of multi-module cavity devices.

system response is simply found by multiplying the corresponding transmission matrices, $\mathbf{T}^{(c)} = \mathbf{T}^{(1)} \times \mathbf{T}^{(2)} \times \dots \times \mathbf{T}^{(N)}$. It is therefore easy to design cavities with complex multi-resonant spectral features. Importantly, the large optomechanical coupling of slotted PhC waveguides [2] enables a large tuning range, which makes it easy to compensate for fabrication imperfections or varying operating conditions. In fact, we show that the mirror modules may be completely reconfigured from a transmissive to a reflective state across a large design bandwidth spanning the entire C-band. To see this, we use a finite-element-method (Comsol Multiphysics) to calculate the deformation of the mirror module in Fig. 1 when a force, F_n , is applied via the comb drives. Fig. 2(a) plots the resulting variation in the slot gap, h_0 , of each PhC unit cell for different values of F_n . Note that the left and right end of the mirror is fixed in order to keep the modules individually programmable. We use a plane-wave expansion method (MPB

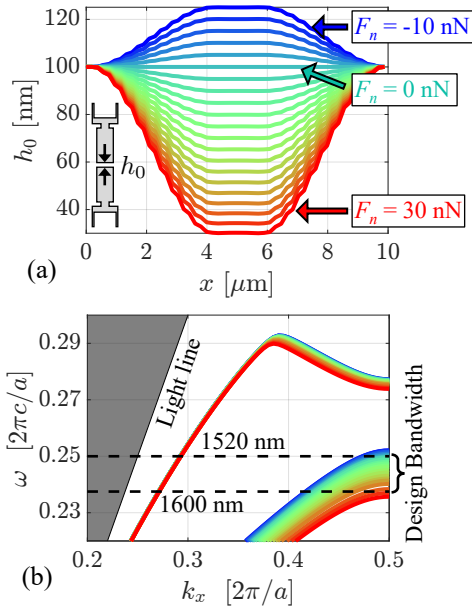


Fig. 2. (a) Deformation of the mirror structure measured via the slot width, h_0 , as a function of location along the x -axis for different forces, F_n . (b) Band diagram simulations for an infinite PhC waveguide with a unit cell corresponding to the central element in (a) at $x \approx 5 \mu\text{m}$. The line colors represent the same values of F_n as in (a) and the design bandwidth (telecom C-band) in indicated by dashed black lines.

- MIT Photonic Bands) to calculate the dispersion relation of an infinite waveguide with properties corresponding to the central unit cell ($x \approx 5 \mu\text{m}$). The results are plotted in Fig. 2(b) and show that the band-edge of the fundamental mode shifts from the short- (1520 nm) to the long (1600 nm) wavelength end of the design bandwidth as the force is increased from 0 to 30 nN. The mirror module therefore changes from transmissive to reflective as the force is increased. Note that only a partial bandgap is created by red-shifting the fundamental dielectric-like mode since the air-like mode is pushed below the light line due to the presence of the "wings" connecting the PhC waveguide to the comb drives.

III. DESIGN EXAMPLE: FOUR-WAVE-MIXING

To demonstrate the power of our design concept, we consider an application example that requires three cavity modes. Degenerate four-wave-mixing (FWM) is a nonlinear optical process that is useful for parametric amplification and photon-pair generation [4]. Using PhC structures is beneficial for reducing both the required pump energy and device footprint, but achieving resonant enhancement requires three modes to be equidistant with a precision given by the resonant linewidths. With our approach, it is easy to design a structure with the desired spectral structure, and the tunability should allow the necessary fine-tuning to achieve exact energy-matching of the FWM process. We use a symmetric structure with three mirrors as illustrated in Fig. 3(a). The two control parameters (F_1 and F_2) are allowed to vary between -10 nN and 30 nN and we find an example solution with $F_1 = 25$ nN and $F_2 = 14.5$ nN with a corresponding transmission spectrum shown

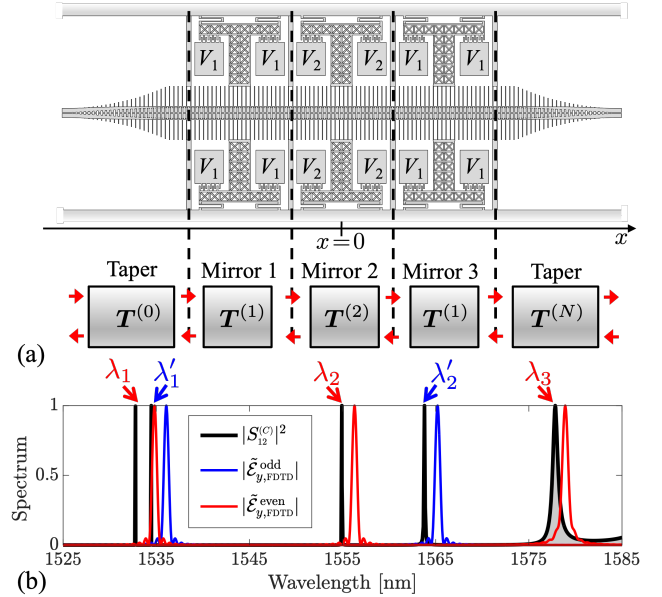


Fig. 3. (a) Sketch of a three-mirror cavity with left-right symmetry. Note that taper sections are used to convert the fundamental PhC waveguide mode into a straight slot waveguide mode. (b) Transmission spectrum calculated using the transfer matrix approach (black). Red (blue) arrows indicate even (odd) parity of the resonant modes with respect to reflections along the symmetry plane $x = 0$. Overlaid in the same plot are spectra calculated from full 3D FDTD simulations imposing even (red) or odd (blue) symmetry.

in Fig. 3(b). To verify the prediction from the transfer matrix approach, we use 3D finite-difference-time-domain (FDTD) simulations to calculate the resonant wavelengths while imposing even (red) or odd (blue) symmetry of the corresponding modes. Fourier transforms of the time traces recorded during the FDTD simulations are also plotted in Fig. 3(b), and we observe a good agreement with deviations in the resonances limited to a few nanometers.

ACKNOWLEDGMENT

This work was funded by the Villum Foundation (QNET-NODES Grant No. 37417).

REFERENCES

- [1] S. Hu, M. Khater, R. Salas-Montiel, E. Kratschmer, S. Engelmann, W. M. J. Green, and S. M. Weiss, "Experimental realization of deep-subwavelength confinement in dielectric optical resonators," *Science Advances*, vol. 4, no. 8, p. eaat2355, 2018.
- [2] L. Midolo, A. Schliesser, and A. Fiore, "Nano-opto-electro-mechanical systems," *Nature Nanotechnology*, vol. 13, no. 1, pp. 11–18, 2018.
- [3] B. V. Lahijani, M. Albrechtsen, R. Christiansen, C. Rosiek, K. Tsoukalas, M. Sutherland, and S. Stobbe, "Electronic-photonic circuit crossings," *arXiv:2204.14257*, 2022.
- [4] G. Marty, S. Combr e, F. Raineri, and A. De Rossi, "Photonic crystal optical parametric oscillator," *Nat. Photonics*, vol. 15, no. 1, pp. 53–58, Jan. 2021.